Calcium, Nucleotide, and Actin Affect the Interaction of Mammalian Myo1c with Its Light Chain Calmodulin†

Alena Lieto-Trivedi and Lynne M. Coluccio*

Boston Biomedical Research Institute, 64 Grove Street, Watertown, Massachusetts 02472

Received June 11, 2008; Revised Manuscript Received July 28, 2008

ABSTRACT: To investigate the interaction of mammalian class I myosin, Myo1c, with its light chain calmodulin, we expressed (with calmodulin) truncation mutants consisting of the Myo1c motor domain followed by 0−4 presumed calmodulin-binding (IQ) domains ($Myo1c^{0IQ}$−$Myo1c^{4IQ}$). The amount of calmodulin associating with the Myo1c heavy chain increased with increasing number of IQ domains from $Myo1c^{0IQ}$ to $Myo1c^{3IQ}$. No calmodulin beyond that associated with $Myo1c^{3IQ}$ was found with $Myo1c^{4IQ}$ despite its availability, showing that Myo1c binds three molecules of calmodulin with no evidence of a fourth IQ domain. Unlike $Myo1c^{0IQ}$, the basal ATPase activity of $Myo1c^{1IQ}$ was >10-fold higher in Ca^{2+} vs EGTA ± exogenous calmodulin, showing that regulation is by Ca^{2+} binding to calmodulin on the first IQ domain. The K_m and V_{max} of the actin-activated Mg^{2+}-ATPase activity were largely independent of the number of IQ domains present and moderately affected by Ca^{2+}. In binding assays, some calmodulin pelleted with Myo1c heavy chain when actin was present, but a considerable fraction remained in the supernatant, suggesting that calmodulin is displaced most likely from the second IQ domain. The Myo1c heavy chain associated with actin in a nucleotide-dependent fashion. In ATP a smaller proportion of calmodulin pelleted with the heavy chain, suggesting that Myo1c undergoes nucleotide-dependent conformational changes that affect the affinity of calmodulin for the heavy chain. The studies support a model in which Myo1c in the inner ear is regulated by both Ca^{2+} and nucleotide, which exert their effects on motor activity through the light-chain-binding region.

Class I myosins are single-headed, actin-associated molecular motors (*1*). Myo1c, one of eight class I myosins expressed in humans, is involved in insulin-mediated translocation of the GLUT4 transporter and functions by promoting membrane fusion of GLUT4-containing vesicles with the plasma membrane (*2, 3*). In the specialized hair cells on the sensory epithelia of the inner ear, Myo1c mediates adaptation of mechanoelectrical transduction, allowing hair cells under prolonged stimuli to stay sensitive to new stimuli (*4*).

Myo1c consists of a motor domain containing the ATP- and actin-binding sites, a light-chain-binding domain (LCBD), and a carboxyl-terminal tail domain. The LCBD contains IQ motifs, which are α-helical segments of 20−25 amino acid residues named for the presence of isoleucine (I) and glutamine (Q) (*5*). As with other class I myosins, the IQ motifs of Myo1c, which are rich in hydrophobic and positively charged residues, bind calmodulin. The current understanding is that mammalian Myo1c contains three IQ motifs, which are occupied by calmodulin in the absence of Ca^{2+} (*6, 7*). The sequences of the first two IQ domains are canonical, whereas the third IQ domain is less well conserved. There is evidence that frog Myo1c contains four IQ domains although the affinity of calmodulin for peptide representing the fourth IQ is low, bringing into question whether it is occupied by calmodulin in Myo1c in the cell (*8*). Whether the LCBD of mammalian Myo1c contains a fourth IQ domain is unknown. The addition of Ca^{2+} causes release of one or more molecules of calmodulin and a decrease in the ability of Myo1c to translocate actin filaments in vitro (*6, 7*) presumably due to destabilization of the lever arm. There is also evidence that dissociation of calmodulin from the LCBD exposes sites for membrane binding in the stereocilia found on hair cells of the inner ear (*9, 10*).

To investigate the number of bona fide calmodulin-binding domains and to understand how calmodulin regulates mammalian Myo1c activity, we have prepared and studied a set of truncation mutants consisting of the Myo1c motor domain ($Myo1c^{0IQ}$) and the Myo1c motor domain with one ($Myo1c^{1IQ}$), two ($Myo1c^{2IQ}$), three ($Myo1c^{3IQ}$), or four ($Myo1c^{4IQ}$) IQ domains. These expressed proteins were analyzed with techniques including calmodulin-binding assays, actin-binding assays, and ATPase assays.

Our studies indicate that mammalian Myo1c binds a maximum of three calmodulins per heavy chain with no compelling evidence of a fourth IQ domain. We find that the motor domain ($Myo1c^{0IQ}$) exhibits no Ca^{2+} sensitivity in its basal ATPase rate; however, $Myo1c^{1IQ}$ displays significant Ca^{2+} sensitivity. We attribute this to a Ca^{2+}-induced conformational change in the calmodulin associated with the first IQ that does not lead to calmodulin dissociation. The results are consistent with a model in which calmodulin binding to the first IQ affects motor domain activity (*11, 12*). We provide supporting evidence that calmodulin from the

† This work was supported by NIH Grants GM68080 and DC008793 to L.M.C. A.L.-T. was the recipient of a Ruth L. Kirschstein National Research Service Award (GM072332).

* Address correspondence to this author. Tel: 617-658-7784. Fax: 617-972-1761. E-mail: coluccio@bbri.org.

10.1021/bi8011059 CCC: $40.75
Published on Web 08/26/2008

FIGURE 1: Alignment by Clustal X and shading by Boxshade of IQ region in Myo1c. Alignment of the sequence immediately following the motor domain of rat Myo1c shows four regions conforming to various degrees to the consensus sequence IQXXXRGXXXR ascribed to the ~23 amino acid in length calmodulin-binding region known as an IQ domain for the presence of isoleucine and glutamine. IQ1 and IQ2 correspond best to the canonical IQ sequence and IQ3 and IQ4 less so.

second IQ dissociates in the presence of Ca^{2+} (*8*). There is little, if any, difference in the actin-activated ATPase activity as a consequence of the presence of the LCBD and associated calmodulins. The results support our previous conclusion that Ca^{2+} affects specific steps in the Myo1c actin-activated ATPase cycle, although not the overall rate (*12*). Actin binding is also not affected by Ca^{2+}; however, binding of Myo1c to actin is nucleotide dependent. We provide evidence that ATP might affect the interaction of calmodulin with the heavy chain.

EXPERIMENTAL PROCEDURES

Preparation of Constructs and Expression in Insect Cells. The region immediately following the motor domain of rat Myo1c was aligned with Clustal X and found to contain four putative IQ regions: two highly conserved, one less well conserved, and one divergent (Figure 1). We designed primers representing the desired start and stop sites and restriction enzyme sites and used them in polymerase chain reactions with the C myr2 tag pBSK vector (kindly supplied by Prof. Martin Bähler) to prepare a series of truncated rat Myo1c constructs representing the motor domain, $Myo1c^{0IQ}$ (amino acids 1−697), and the motor domain with either the first IQ domain, $Myo1c^{1IQ}$ (amino acids 1−725), first and second IQ domains, $Myo1c^{2IQ}$ (amino acids 1−749), first, second, and third IQ domains, $Myo1c^{3IQ}$ (amino acids 1−774), or first through fourth IQ domains, $Myo1c^{4IQ}$ (amino acids 1−798) (Figure 2A). The constructs were terminated a few amino acids after the predicted end of the IQ domains to foster calmodulin binding to the terminal IQ domain (Figure 2B). The FLAG tag (DYKDDDDK) was incorporated at the carboxyl terminus to allow for affinity purification. The resulting PCR products were treated with the appropriate restriction enzymes and then ligated into the appropriately cut pFastBacDUAL transfer vector (Gibco BRL, Gaithersburg, MD) downstream of the polyhedrin promoter; the p10 promoter cloning site contained the gene coding for calmodulin (*13*). The plasmids were transformed into DH5α *Escherichia coli* cells, and colonies were selected based on antibiotic resistance. Colonies were grown, and the isolated DNA was tested for the presence of inserts by restriction analysis. The recombinant donor plasmids were transformed into DH10Bac *E. coli* cells (Invitrogen, Carlsbad, CA) for transposition into the bacmid. Recombinant bacmid DNA was isolated by potassium acetate precipitation as described by the Bac-to-Bac Baculovirus Expression Systems Instruction Manual supplied by the manufacturer. Virus was produced by transfecting the recombinant bacmid DNA into *Spondoptera frugiperda* 9 (Sf9) insect cells with Cellfectin reagent (Invitrogen) followed by 3 days of growth. Subsequently, amplified virus was used to infect Sf9 cells in suspension. In the case of $Myo1c^{2IQ}$, $Myo1c^{3IQ}$, and $Myo1c^{4IQ}$, cells were cotransfected with calmodulin virus to ensure sufficient calmodulin availability. Infection was allowed to proceed for 4 days after which time cells were harvested by centrifugation. Cell pellets were either used immediately for protein isolation or frozen in liquid N_2 and stored at −80 °C for future use.

Protein Purification. The Myo1c fragments were isolated using a previously described method (*14*). Briefly, the insect cell pellets were homogenized in 10 mM Tris, pH 7.5, 0.2 M NaCl, 4 mM $MgCl_2$, and 2 mM ATP in the presence of protease inhibitors and then centrifuged at 45000 rpm for 50 min. The supernatant was applied to an anti-FLAG column, and after washing, the expressed proteins were eluted with a step gradient from 0 to 120 μg/mL FLAG peptide. Fractions containing protein were analyzed by SDS−PAGE[1], and the fractions containing highly purified protein were pooled and dialyzed against 10 mM Tris, pH 7.5, 50 mM KCl, and 1 mM DTT. Proteins were either used immediately or stored at −80 °C for future use.

^{125}I-Calmodulin Overlays. Bacterially expressed human calmodulin prepared as previously described (*15, 16*) was radiolabeled with iodine using Bolton−Hunter reagent (*17*). ^{125}I-Calmodulin overlays were performed according to the method of Glenney and Glenney (*18*). ^{125}I-Calmodulin was added to blocking solution containing 3% bovine serum albumin and either 0.2 mM $CaCl_2$ or 1 mM EGTA. $Myo1c^{0IQ}$−$Myo1c^{4IQ}$ proteins were transferred from a SDS−polyacrylamide gel to nitrocellulose. The nitrocellulose was treated with blocking solution and incubated with ^{125}I-calmodulin ± Ca^{2+} at 37 °C for 3−4 h. After washing with Tris-buffered saline containing 0.2% Tween-20, the nitrocellulose was exposed to film.

ATPase Assays. ATPase activity was evaluated using a colorimetric assay that measures phosphate (*19*). Standard curves were generated with known amounts of phosphate. The assay was performed at 37 °C in 10 mM Tris, pH 7.5, 50 mM KCl, 1 mM DTT, 1 mM $MgCl_2$, 1 mM ATP, and the appropriate ratio of 2 mM EGTA to 2 mM CaEGTA to effect pCa values of 4.6 or 8.9 (*14*). To determine K_m and V_{max}, the data were fit to hyperbolas using Origin 7 (Microcal, Northampton, MA). For actin-activated ATPase assays, phalloidin-stabilized actin was used at 0−75 μM. In addition to the pCa 4.6 and 8.9 conditions, basal ATPase activity was investigated in samples prepared at pCa 4.6 followed by the addition of EGTA to effect pCa 8.9 before assaying. Basal activity of $Myo1c^{1IQ}$ was also measured under each condition in the presence of 15 μM exogenous calmodulin.

Actin Cosedimentation Assays. Binding of the truncated Myo1c molecules and associated calmodulin to filamentous rabbit skeletal muscle actin, at varying Ca^{2+} concentrations, was studied using actin cosedimentation assays as previously described (*20*). The assays were done in 10 mM Tris, pH 7.5, 50 mM KCl, 1 mM DTT, 1 mM $MgCl_2$, ± 5 mM ATP, 0−70 μM calmodulin depending on the experiment, and 0.1 mM $CaCl_2$ (pCa 4) or 2 mM EGTA (pCa 8.9). When present, exogenous calmodulin was incubated with myosin for 10 min on ice before addition of actin. Five micromolar

[1] Abbreviation: SDS−PAGE, sodium dodecyl sulfate−polyacrylamide gel electrophoresis.

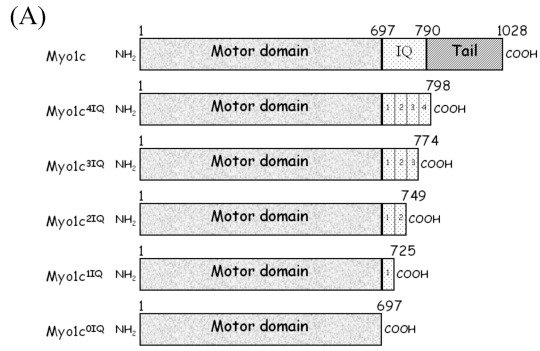

FIGURE 2: Schematic and sequences of the constructs used in this study. Domain structure of full-length Myo1c, followed by the five constructs used in this study (A). Partial sequences of the constructs used; in each case the predicted IQ region (underlined) is followed by 5−8 amino acids to foster calmodulin binding to the terminal IQ domain (B). All constructs were FLAG-tagged at the carboxyl terminus to allow for affinity purification.

filamentous actin and ~0.5−0.7 μM truncated Myo1c were incubated for 30 min on ice. The samples were then centrifuged at 239000*g* for 20 min at 4 °C. Supernatants were removed and precipitated with 10% trichloroacetic acid. The precipitated proteins were then collected, solubilized in 1 M Tris base, and prepared for SDS−PAGE. Pellets were directly solubilized in 1 M Tris base followed by the addition of sample buffer for SDS−PAGE.

Data Analysis. The relative amounts of myosin and calmodulin on all Coomassie-stained gels were determined by densitometry using the Odyssey Infrared Imaging System (LI-COR Biosciences, Lincoln, NE). For actin cosedimentation assays, the ratios of calmodulin to heavy chain in the pellet in the presence of actin were calculated after subtraction of the amount of protein that pelleted in the absence of actin. Densitometry of the ^{125}I-calmodulin overlays was analyzed with Scion Image (Scion Corp., Frederick, MD), which is based on NIH Image.

Other. Rabbit skeletal muscle actin was prepared as previously described (*21*). Homogeneous fractions, as determined by SDS−PAGE, were pooled, polymerized by the addition of 50 mM KCl, 1 mM $MgCl_2$, and 1 mM ATP, then aliquoted into cryotubes before freezing in liquid N_2, and stored at −80 °C until use.

RESULTS

Association of Calmodulin with Expressed Myo1c Mutants. We expressed in insect cells and purified by affinity chromatography FLAG-tagged truncated forms of Myo1c consisting of the motor domain followed by 0−4 predicted IQ domains along with calmodulin (Figure 3A). With the exception of Myo1c^{0IQ}, calmodulin copurified with each of the heavy chains. Densitometry of the expressed proteins indicated that the amount of calmodulin associated with Myo1c^{3IQ} > Myo1c^{2IQ} > Myo1c^{1IQ} > Myo1c^{01Q}, but no significant difference in the amount of associated calmodulin between Myo1c^{3IQ} and Myo1c^{4IQ} was detected (Figure 3B). Using standard curves of expressed bovine calmodulin and Myo1c^{0IQ}, we predict that Myo1c^{1IQ} has approximately 1 mol of calmodulin, Myo1c^{2IQ} has ~2 mol of calmodulin, and both Myo1c^{3IQ} and Myo1c^{4IQ} have 2−3 mol of calmodulin per mole of heavy chain (Table 1).

Calmodulin Binding to Myo1c Mutants. In I^{125}-calmodulin overlays, which rely on the ability of the transferred immobilized protein to renature at least partially, the Myo1c mutants with the exception of Myo1c^{0IQ} bound radiolabeled calmodulin. Binding to each of the mutants with IQ domains was stronger in 1 mM EGTA (Figure 4B) vs 0.2 mM $CaCl_2$ (Figure 4A). As most noticeable in Ca^{2+}, calmodulin binding increased as a function of the number of predicted IQ domains present until Myo1c^{3IQ} (Figure 4A). Only a minor increase in signal from Myo1c^{3IQ} to Myo1c^{4IQ} suggests that if a fourth IQ exists, it binds calmodulin very weakly, if at all, under these conditions (Figure 4C).

Solubility of Expressed Proteins. The purified truncated Myo1c proteins were centrifuged at high speed to investigate their solubility (Figure 5). Myo1c^{0IQ}, Myo1c^{1IQ}, Myo1c^{2IQ}, and Myo1c^{3IQ} were largely soluble after centrifugation in 10 mM Tris, pH 7.5, 50 mM KCl, and 1 mM DTT at 239000*g* for 20 min at 4 °C. In contrast, the majority (~72%; Figure 5B) of Myo1c^{4IQ} pelleted at high speed, indicating that the protein is largely insoluble. A much higher percentage of calmodulin relative to heavy chain is found in the supernatant of Myo1c^{4IQ} after the spin, indicating that some calmodulin dissociated from the heavy chain that pelleted (Figure 5B).

ATPase Assays. ATPase assays were performed with the Myo1c constructs after removal of insoluble protein by centrifugation. In the absence of actin, the basal ATPase activity of Myo1c^{0IQ} was unaffected by Ca^{2+}. In contrast, the basal ATPase activity of the other constructs was significantly lower (>10-fold) at pCa 8.9 (1 nM free Ca^{2+}) than at pCa 4.6 (25 μM free Ca^{2+}) (Table 2). Results with Myo1c^{1IQ} show that the Ca^{2+} effect on the basal activity is

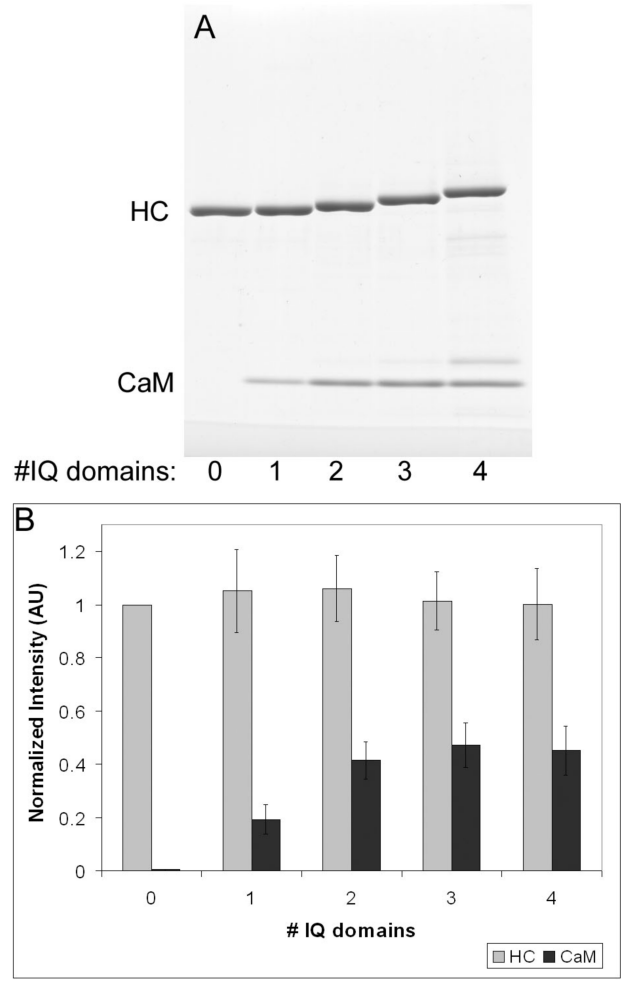

FIGURE 3: Purified Myo1c constructs and associated calmodulin. Myo1c constructs with 0, 1, 2, 3, or 4 IQ domains were purified from insect cells by affinity purification. The relative amounts of associated calmodulin (CaM) and Myo1c heavy chain (HC) are shown in (A), with quantification by densitometry shown in (B). The error bars are standard deviations of normalized intensity measurements from three gels.

Table 1: Molar Ratio of Calmodulin to Myosin Heavy Chain[a]

	molar ratio (CaM/HC)
Myo1c^{0IQ}	0
Myo1c^{1IQ}	0.9 ± 0.1
Myo1c^{2IQ}	2.0 ± 0.4
Myo1c^{3IQ}	2.5 ± 0.6
Myo1c^{4IQ}	2.4 ± 0.4

[a] Data are averages from two CaM and Myo1c^{0IQ} standard curves; uncertainties are standard deviations.

attributable to calmodulin associated with the first IQ. To investigate whether the Ca^{2+} effect could be due to calmodulin dissociation from the first IQ, the experiment was repeated in the presence of 15 μM exogenous calmodulin (Table 3). The high basal activity of Myo1c^{1IQ} in Ca^{2+} was still observed. Furthermore, if the pCa was changed from 4.6 to 8.9 with the addition of EGTA, the ATPase activity was not different from samples treated at pCa 8.9, suggesting that the effects of Ca^{2+} are reversible (Table 3). One interpretation is that although Ca^{2+} induces conformational changes in calmodulin associated with the first IQ domain, it does not lead to its dissociation (see Discussion).

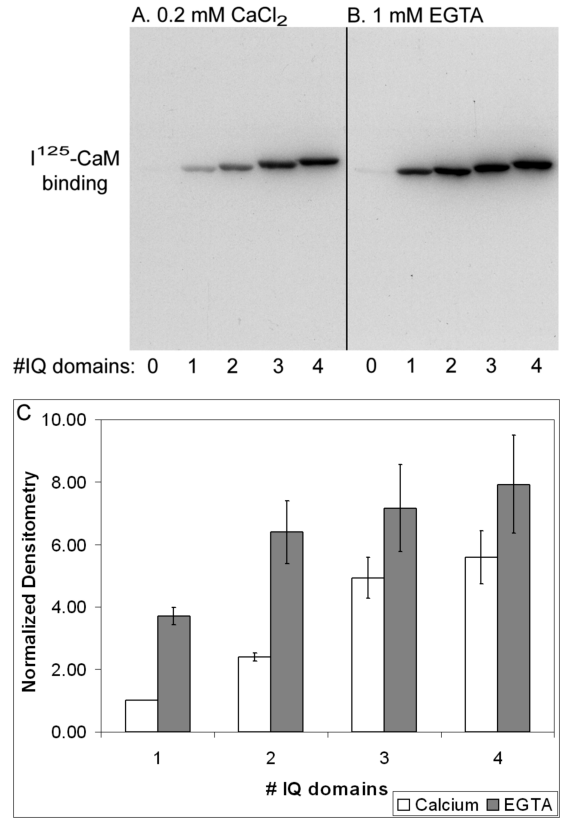

FIGURE 4: ^{125}I-Calmodulin overlays demonstrate association of calmodulin with immobilized Myo1c constructs. Radiolabeled calmodulin (CaM) binding in the presence of 0.2 mM $CaCl_2$ (A) or 1 mM EGTA (B). Normalized densitometry shows increased binding in EGTA (gray) compared to Ca^{2+} (white) (C). More noticeable in Ca^{2+}, there was an increase in calmodulin binding with the number of IQ domains present from Myo1c^{1IQ} to Myo1c^{3IQ}. Representative blots are shown in panels A and B. Densitometry values from four different exposures were normalized to Myo1c^{1IQ} in $CaCl_2$, averaged, and plotted in panel C; error bars represent standard deviations. The experiment was repeated several times with the same results.

For the actin-activated ATPase assays, roughly equivalent amounts of protein ($\sim$0.6$-$0.8 μg) were used in each case with the exception of Myo1c^{4IQ}, which was available only in smaller amounts because of its insolubility. In that case $\sim$0.12 μg were used per assay (Figure 6A). The V_{max} of the actin-activated Mg^{2+}-ATPase activity of the constructs in Ca^{2+} ranged from 2.4 s^{-1} (Myo1c^{4IQ}) to 5.0 s^{-1} (Myo1c^{2IQ}) (Table 2). Myo1c^{0IQ} (Figure 6B) showed no Ca^{2+} sensitivity, whereas the V_{max} of both Myo1c^{1IQ} (Figure 6C) and Myo1c^{2IQ} (Figure 6D) decreased at pCa 8.9, while the K_m remained roughly the same. The K_m of both Myo1c^{3IQ} (Figure 6E) and Myo1c^{4IQ} (Figure 6F) increased slightly in EGTA (Table 2).

Actin Cosedimentation Assays. The interaction of the Myo1c constructs with actin filaments $\pm$ ATP was determined with cosedimentation assays with and without exogenous calmodulin at both pCa 4 and 8.9. As controls, in all cases the Myo1c constructs were centrifuged under the specified conditions in the absence of actin. The majority of the Myo1c^{1IQ}, Myo1c^{2IQ}, and Myo1c^{3IQ} heavy chains and associated calmodulin were soluble in the absence of actin regardless of the Ca^{2+} or nucleotide concentration (e.g., Figure 8C). The presence of exogenous calmodulin resulted in a slight decrease in the amount of heavy chain in the pellet in the absence of actin (data not shown). ATP also caused a

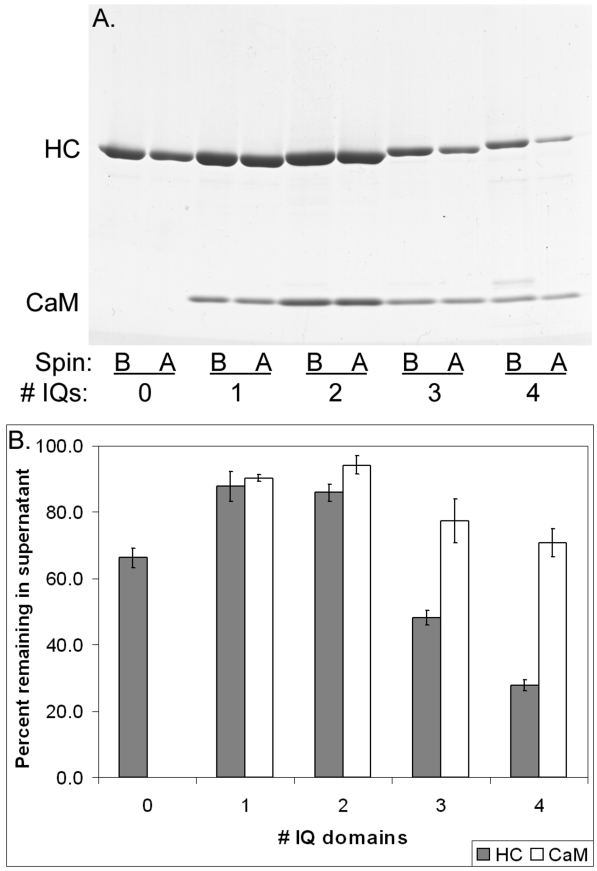

FIGURE 5: Solubility of Myo1c constructs. The amount of Myo1c heavy chain (HC) and calmodulin (CaM) in solution is shown in panel A before ("B") and after ("A") a high-speed spin of $Myo1c^{0IQ}$−$Myo1c^{4IQ}$ in 10 mM Tris, pH 7.5, 50 mM KCl, and 1 mM DTT. The most significant change was seen for $Myo1c^{4IQ}$, with the majority of the protein pelleting under these conditions. The percentage of each heavy chain (gray) and calmodulin (white) remaining in the supernatant after the spin is plotted in panel B. Values represent averages from three gels; error bars represent standard deviations. For $Myo1c^{4IQ}$, the much higher percentage of CaM remaining in the supernatant relative to HC indicates that the heavy chain is largely insoluble. The insolubility of $Myo1c^{4IQ}$ was observed with multiple protein preparations.

slight decrease in the amount of $Myo1c^{1IQ}$ and $Myo1c^{2IQ}$ heavy chain in the pellet in the absence of actin (Figure 8A,C). The solubility of $Myo1c^{4IQ}$ was limited. We considered the possibility that the absence of calmodulin in association with the putative fourth IQ domain is responsible for the insolubility; however, the addition of 100 μM exogenous calmodulin did not significantly increase solubility (data not shown). Alternatively, this region constitutes a binding site for another protein (see Discussion).

In the presence of actin nearly all of the $Myo1c^{1IQ}$, $Myo1c^{2IQ}$, and $Myo1c^{3IQ}$ heavy chain and calmodulin cosedimented at pCa 4 in the absence of ATP; however, a fraction of the total calmodulin remained in the supernatant (Figure 7A−C). This fraction was negligible in the case of $Myo1c^{1IQ}$, with more significant amounts of calmodulin remaining in the supernatants of the longer forms (Figure 7A, lanes 1, 3, and 5). The supernatants of $Myo1c^{2IQ}$ and $Myo1c^{3IQ}$ contained roughly 30−40% of the total calmodulin in the sample, suggesting that one molecule of calmodulin was released per heavy chain, most likely from the second IQ position (Figure 7C, white bars; see Discussion). These results did not vary significantly at pCa 8.9, although there was a slightly smaller percentage of total calmodulin in the supernatant compared to pCa 4, consistent with a tighter calmodulin−IQ domain interaction in EGTA (data not shown). The addition of exogenous calmodulin resulted in roughly a 10−30% increase in the amount of calmodulin relative to heavy chain associated with actin (Figure 7B,D). In a separate assay, the addition of up to 70 μM exogenous calmodulin to $Myo1c^{4IQ}$ did not increase the amount of calmodulin per heavy chain above that observed with $Myo1c^{3IQ}$ (data not shown), giving further evidence that Myo1c contains three bona fide calmodulin-binding regions.

In the presence of 5 mM ATP, ~20−40% of the total $Myo1c^{1IQ}$, $Myo1c^{2IQ}$, and $Myo1c^{3IQ}$ heavy chain present pelleted with actin essentially independent of the Ca^{2+} concentration; however, in ATP only ~10% of the total calmodulin was observed in the pellet (Figure 8B,C). Also noteworthy is that although the solubility of the $Myo1c^{3IQ}$ heavy chain did not vary in the presence of ATP (Figure 8A,C), the amount of calmodulin associated with the heavy chain in the pellet decreased by roughly half in ATP. The ratio of calmodulin to heavy chain associated with actin decreased in the presence of ATP (Figure 8D), most significantly for $Myo1c^{3IQ}$. The results indicate that the nucleotide state of the motor domain promotes dissociation of calmodulin.

Coimmunoprecipitation of Calmodulin with Myo1c Mutants. We used coimmunoprecipitation experiments with anti-FLAG beads to analyze the association of calmodulin with the Myo1c constructs in the absence of actin ± Ca^{2+}; however, the results were difficult to interpret due to technical problems. Briefly, Myo1c was incubated with anti-FLAG beads and then, following several washes, was eluted by the addition of FLAG peptide. More $Myo1c^{1IQ}$, $Myo1c^{2IQ}$, and $Myo1c^{3IQ}$ heavy chain and associated calmodulin consistently eluted from the beads in EGTA, but it was difficult to determine whether this was due to an effect on the interaction between the myosin and the anti-FLAG beads or on myosin solubility (data not shown). The relative amount of associated calmodulin did not differ as a function of Ca^{2+} concentration. In the case of $Myo1c^{4IQ}$, no detectable heavy chain or calmodulin eluted from the beads, likely due to the large degree of insolubility. To determine if exogenous calmodulin results in reassociation of calmodulin, we incubated the Myo1c constructs with exogenous calmodulin prior to affinity purification. $Myo1c^{2IQ}$ and $Myo1c^{3IQ}$ showed no significant effect in the ratio of calmodulin to heavy chain in the presence of exogenous calmodulin; however, more heavy chain and calmodulin eluted from the beads in the presence of exogenous calmodulin both in Ca^{2+} and in EGTA (data not shown). This might indicate that the presence of excess calmodulin increases the solubility of the heavy chain.

DISCUSSION

Previous studies showed that mammalian Myo1c contains three calmodulin-binding regions (*22*−*24*). In addition, Ca^{2+} causes dissociation of calmodulin from Myo1c and a decrease in the in vitro motility of actin filaments, most likely by destabilization of the lever arm (*7*). From two studies using peptides containing the Myo1c IQ domains, (i) IQ1 from mouse Myo1c was determined to have the highest affinity (relative to IQ2 and IQ3) for calmodulin in the absence of

Table 2: ATPase Activity[a]

pCa	Myo1c^{0IQ}	Myo1c^{1IQ}	Myo1c^{2IQ}	Myo1c^{3IQ}	Myo1c^{4IQ}
			V_0 (s^{-1}) Basal Activity in Absence of Actin		
4.6	0.155 ± 0.003	0.295 ± 0.017	0.265 ± 0.001	0.49 ± 0.07	0.305 ± 0.015
8.9	0.136 ± 0.007	0.013 ± 0.006	0.013 ± 0.001	0.051 ± 0.005	0.08 ± 0.06
			V_{max} (s^{-1}) Actin-Activated Activity		
4.6	4.48 ± 0.07	3.4 ± 0.2	5.0 ± 0.6	3.3 ± 0.4	2.43 ± 0.08
8.9	4.1 ± 0.4	2.8 ± 0.2	3.5 ± 0.6	3.9 ± 0.5	3.4 ± 0.6
			K_m (μM) Actin Concentration at Half V_{max}		
4.6	37 ± 1	23 ± 4	43 ± 10	25 ± 9	20 ± 2
8.9	34 ± 8	27 ± 6	36 ± 13	42 ± 12	58 ± 19

[a] V_0 data are averages of duplicate measurements in a single assay; uncertainties are standard deviations. V_{max} and K_m are obtained from hyperbolic fits of ATPase data after subtraction of basal activity; uncertainties are obtained from fit results.

Table 3: Basal ATPase Activity[a]

	V_0 (s^{-1}) ATPase activity in absence of actin			
pCa	Myo1c^{0IQ}	Myo1c^{1IQ}	Myo1c^{1IQ} + CaM	Myo1c^{2IQ}
4.6	0.197 ± 0.011	0.338 ± 0.007	0.342 ± 0.012	0.349 ± 0.002
8.9	0.19 ± 0.02	0.024 ± 0.001	0.029 ± 0.001	0.026 ± 0.001
4.6−8.9	0.166 ± 0.001	0.028 ± 0.001	0.026 ± 0.002	0.035 ± 0.003

[a] Data are averages of duplicate measurements in a single assay; uncertainties are standard deviations. Data at pCa 4.6−8.9 represent samples prepared at pCa 4.6, followed by the addition of EGTA before measuring activity.

Ca^{2+} and the lowest affinity in the presence of Ca^{2+} (*11*), and (ii) frog Myo1c was shown to contain a fourth IQ region although with considerably less affinity for calmodulin (*8*).

In our hands, results from surface plasmon resonance and isothermal calorimetry studies with peptides representing the four putative IQ domains of rat Myo1c, singly or in combination, were not reproducible, likely a consequence of the insolubility of the peptides and/or nonspecific binding (data not shown). An additional factor pointing to the need for an alternative approach to investigate calmodulin binding to the IQ domains vs peptide studies came from modeling studies. The span of each IQ domain in Myo1c is small (23 amino acids), and molecular modeling predicts that the LCBD must be essentially straight in order for calmodulins to bind in tandem (*25*). The ramification of this tight fit is that the interaction of calmodulin with a particular IQ domain will be affected by the presence of adjacent calmodulins. In addition, binding of calmodulin to the first IQ domain is predicted to be affected by the motor domain as the converter region in the motor domain translates information from the actin- and nucleotide-binding sites to the rest of the molecule (*25, 26*). Given these concerns, we carried out studies with truncated mutants to investigate the number of calmodulin-binding domains in rat Myo1c, the interaction of calmodulin with the LCBD, and the effect of Ca^{2+} and ATP on binding of Myo1c and its associated calmodulin to actin. The truncated mutants express at very high levels facilitating experimentation.

This study uses a set of Myo1c constructs consisting of the motor domain and ending after zero, one, two, three, or four predicted IQ domains (Figure 2A). Not surprisingly, we found that the truncation point was important. Only minor amounts of calmodulin were found with the 1IQ form from a set of Myo1c constructs terminating immediately following the last amino acid of the terminal IQ domain. As a result, the constructs used in this study were redesigned to terminate 5−8 amino acids after the predicted end of the terminal IQ domain (Figure 2B). The extension beyond the end of the last IQ domain of interest permitted calmodulin binding presumably by allowing proper secondary structure of the LCBD to be assumed.

The expressed Myo1c isoforms purify with increasing proportions of calmodulin per heavy chain until 3IQ domains are present (Figure 3). There is no further increase in calmodulin with the addition of the fourth IQ domain. Both Myo1c^{3IQ} and Myo1c^{4IQ} contain 2−3 calmodulins per heavy chain (Table 1), which is consistent with previous findings (*8, 11*). Gillespie and Cyr (*8*) used hydrodynamic analysis of full-length bullfrog Myo1c and a construct including the IQ domains plus the tail of Myo1c to determine the calmodulin to heavy chain stoichiometry. They found ~2−3 calmodulins per heavy chain in both Ca^{2+} and EGTA at 4 °C. Manceva et al. (*11*) found three calmodulins per heavy chain bound to a construct of the mouse Myo1c motor domain plus the first three IQ domains ± Ca^{2+} at 25 °C using actin sedimentation assays and densitometry. The construct used in the Manceva et al. study is similar to the Myo1c^{3IQ} used in this study, although it was terminated only one residue after the end of the third IQ, compared to Myo1c^{3IQ}, which includes seven additional amino acids. Although our results cannot rule out conclusively the possibility that calmodulin associates with the fourth IQ *and* its occupancy results in dissociation of calmodulin from one of the other IQ domains, the low sequence homology of the presumed fourth IQ domain suggests otherwise. In addition, the concentration of free calmodulin in hair cells is predicted to be 35 μM, which suggests that, in the cell, the fourth IQ could not be occupied with calmodulin (*27*).The increase in calmodulin with increasing number of IQ domains was supported by overlays with radiolabeled calmodulin (Figure 4). We also found that calmodulin associated with the heavy chains to a greater extent in the presence of EGTA vs $CaCl_2$. This observation is consistent with previous findings that Ca^{2+} causes dissociation of one or more calmodulins from Myo1c (*7, 8, 11*).

We found no compelling evidence for a fourth calmodulin-binding domain as proposed from peptide studies to be present in bullfrog Myo1c (*8*). It is worth noting that there are sequence differences between bullfrog and rat Myo1c IQ domains, which might account for this. Another possibility is that calmodulin is unable to bind to the fourth IQ domain when it is adjacent to the other three domains, as in our Myo1c^{4IQ} construct, possibly due to steric constraints

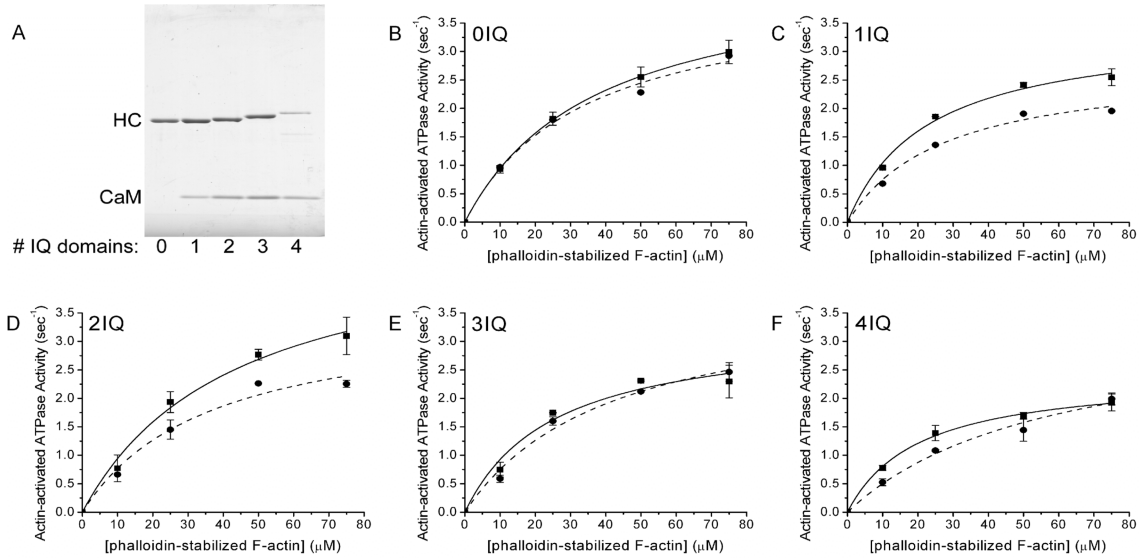

FIGURE 6: Actin-activated Mg^{2+}-ATPase activity of Myo1c constructs. The amount and quality of each protein used in ATPase assays are shown (A). The actin-activated Mg^{2+}-ATPase activity of the Myo1c constructs used in this study is plotted as a function of actin concentration at pCa 4.6 (solid lines with square data points) and 8.9 (dashed lines with circular data points) (B−F). The curves are best described as hyperbolas. $Myo1c^{1IQ}$ and $Myo1c^{2IQ}$ show some calcium sensitivity. The K_m and V_{max} for each are indicated in Table 2. The data represent the average of two samples; the error bars represent standard deviation.

(*25*). In mouse Myo1c, which has significant sequence homology to rat including the IQ region, there is recent evidence that calcium-binding protein 1 (CaBP1) competes with calmodulin for binding to the first three IQ domains in the presence of Ca^{2+}. CaBP1 also shows some binding affinity for the putative fourth IQ domain (*28*).

Our results show that the basal ATPase activity of $Myo1c^{1IQ}$ is >10-fold higher at pCa 4.6 vs 8.9, demonstrating that the presence of the first IQ domain confers Ca^{2+} sensitivity on the motor domain (Tables 2 and 3). One notion is that this change in activity is a consequence of Ca^{2+}-induced dissociation of calmodulin from the first IQ; however, the same effect on the basal ATPase activity was observed in the presence of excess calmodulin, suggesting that this is not the case (Table 3). These results are not easily reconciled with studies with peptides showing that in Ca^{2+} calmodulin dissociates rapidly from IQ1 (*11*). It is also possible that the conformation calmodulin adopts on IQ1 in Ca^{2+} is distinct from that in EGTA, although still remains attached. Structural evidence shows that the N- and C-lobes of calmodulin adopt different conformations referred to as open, semiopen, or closed (*25*). In addition, the light chains of myosin V adopt either a compact conformation in which both N- and C-lobes bind the IQ motif or an extended conformation in which the N-lobe does not interact with the IQ motif (*29*).

The actin-activated ATPase results presented here are consistent with our recent collaborative study, which determined that the steady-state actin-activated ATPase activity of $Myo1c^{1IQ}$ shows little Ca^{2+} sensitivity (*12*). In the Adamek study, however, the ATP hydrolysis step was found to be inhibited 7-fold and ADP release was accelerated 10-fold in Ca^{2+} (*12*), indicating that Ca^{2+} exerts its effect by modifying specific steps in the ATPase cycle. We have also previously shown that Ca^{2+}-dependent changes in enzymatic activity of Myo1b are also attributable to Ca^{2+} binding to calmodulin associated with the first IQ motif (*13*).

There was no significant difference in the association of the Myo1c constructs with actin or the ratio of calmodulin to Myo1c heavy chain as a function of Ca^{2+} concentration from pCa 4 to 8.9. The presence of extra calmodulin results in a slight increase in the proportion of calmodulin to heavy chain that pellets with actin in sedimentation assays (Figure 7D). Manceva et al. (*11*) saw similar results in sedimentation assays of a mouse Myo1c construct containing 3IQ domains. Similarly, in coimmunoprecipitation studies, the only observable effect of Ca^{2+} or exogenous calmodulin was to modify the amount of Myo1c that eluted from anti-FLAG beads. The ratio of calmodulin to Myo1c heavy chain was not noticeably affected. These results indicate that the Myo1c constructs contain a full complement of calmodulin. Alternatively, if they do not have a full complement, exogenous calmodulin is unable to reassociate with the truncated heavy chain perhaps due to structural considerations.

There was no detectable $Myo1c^{1IQ}$, $Myo1c^{2IQ}$, or $Myo1c^{3IQ}$ heavy chain remaining in the supernatant after cosedimentation with actin at pCa 4 in the absence of ATP. However, a fraction of the total calmodulin remained in the supernatants of $Myo1c^{2IQ}$ and $Myo1c^{3IQ}$ (Figure 7A,C). Since the amount of calmodulin in the supernatant of $Myo1c^{1IQ}$ was negligible, this implies that calmodulin dissociates from the second IQ domain more readily than the first. Gillespie and Cyr (*8*) proposed that calmodulin is most likely to dissociate from IQ2 first since this would relieve any strain associated with having three adjacent calmodulins bound to the neck region.

ATP slightly increased the solubility of $Myo1c^{1IQ}$ and $Myo1c^{2IQ}$, resulting in less protein pelleting in sedimentation assays in the absence of actin (Figure 8A,C). The presence of ATP also decreased the ratio of calmodulin to heavy chain in the pellet, indicating that there could be ATP-induced dissociation of calmodulin from the IQ region (Figure 8D). Studies designed to investigate nucleotide-induced changes in the conformation of Myo1c are ongoing (C.-F. Song, L. M. Coluccio, and J. Trinick, personal communication).

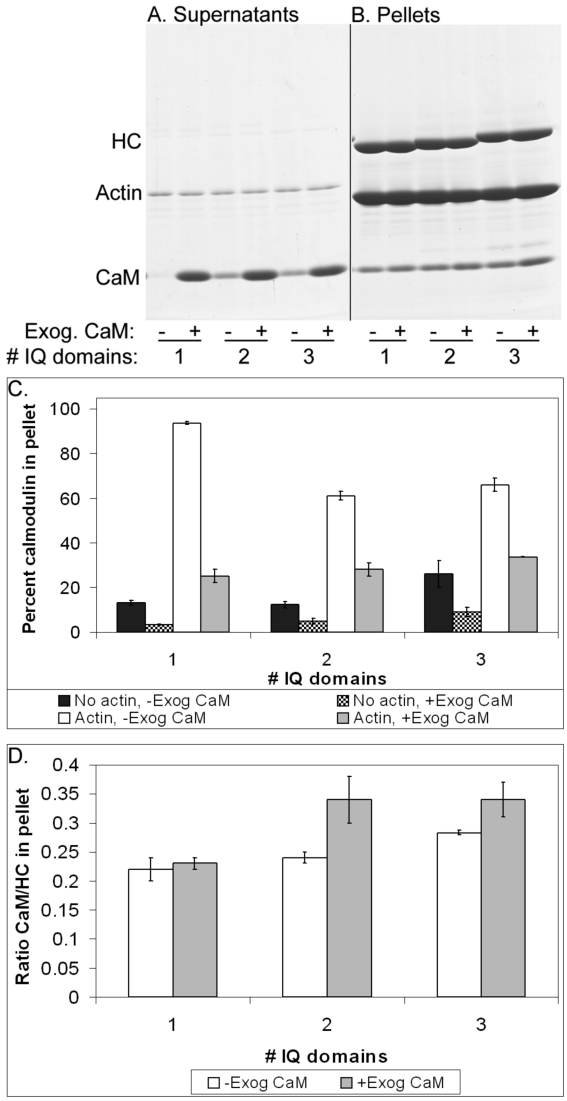

FIGURE 7: Actin sedimentation assay with exogenous calmodulin. Myo1c^{1IQ}, Myo1c^{2IQ}, and Myo1c^{3IQ} (~5.5 μg each) were cosedimented with 5 μM F-actin at pCa 4 in the absence of ATP, ± 3.5 μM exogenous calmodulin. Supernatants (A) and pellets (B) from one assay are shown. Most of the heavy chain (HC) pellets with actin; some calmodulin (CaM) dissociates and appears in the supernatants of Myo1c^{2IQ} and Myo1c^{3IQ}. Panel C displays the percent of total calmodulin in the pellet without actin in the absence (dark gray) and presence (checkered) of exogenous CaM; and with actin in the absence (white) and presence (light gray) of exogenous CaM. Panel D shows the ratio of calmodulin to heavy chain in the pellet associated with actin in the absence (white) and presence (light gray) of exogenous CaM. In panels C and D values are averages of densitometry from duplicate experiments, and error bars represent standard deviations. See Results for details.

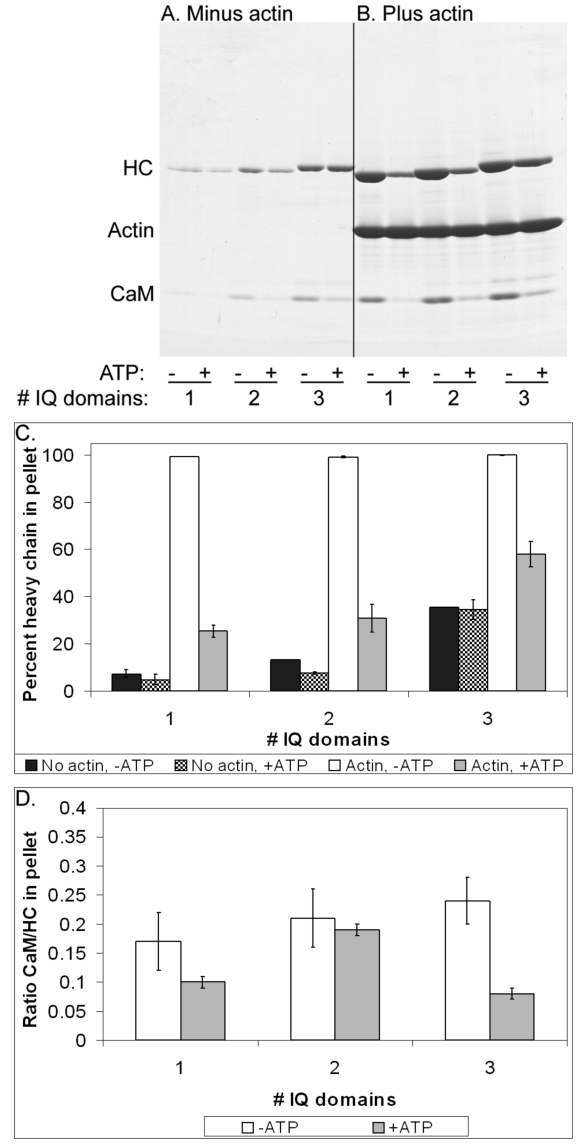

FIGURE 8: Actin sedimentation assay with ATP. Myo1c^{1IQ}, Myo1c^{2IQ}, and Myo1c^{3IQ} (~5.25 μg each) were cosedimented with 5 μM F-actin at pCa 4 ± 5 mM ATP. Pellets in the absence (A) and presence (B) of F-actin from one assay are shown. Panel C displays the percent of total heavy chain in the pellet without actin in the absence (dark gray) and presence (checkered) of ATP; and with actin in the absence (white) and presence (light gray) of ATP. Panel D shows the ratio of calmodulin (CaM) to heavy chain (HC) in the pellet associated with actin in the absence (white) and presence (light gray) of ATP. In panels C and D values are averages of densitometry from duplicate experiments, and error bars represent standard deviations. For Myo1c^{1IQ} and Myo1c^{2IQ}, ATP results in a slight decrease in the amount of heavy chain in the pellet in the absence of actin. In all cases, ATP decreases the proportion of calmodulin to heavy chain in the pellet, indicating CaM dissociation. See Results for details.

The results have implications for the role of Myo1c as the adaptation motor in the inner ear. Neighboring stereocilia on hair cells are connected by extracellular links associated with transduction channels. The current thinking is that an adaptation motor complex, comprised of Myo1c molecules, is associated with the channels and the actin cytoskeleton and responds to changes in tension on the tip links (*4*). Deflection of the stereocilia as a consequence of sound or motion causes an increase in intracellular Ca^{2+}. Ca^{2+} causes Myo1c to dissociate from actin filaments and slip down the actin cytoskeleton. Then, when the tension on the tip links is reduced, Myo1c ascends the actin cytoskeleton reestablishing the resting potential. Our results are consistent with a model in which the effects of Ca^{2+} are a consequence of its effects on specific steps in the ATPase cycle rather than through modification of the LCBD (*12*). Furthermore, we predict that the observed Ca^{2+} effects on enzymatic activity of Myo1c are a consequence of Ca^{2+}-induced changes in calmodulin in association with the first IQ, not necessarily leading to calmodulin dissociation. Our results support the notion, however, that calmodulin dissociates from the *second* IQ, which could provide a binding site for a stereociliary receptor as previously proposed (*9*).

ACKNOWLEDGMENT

We appreciate the able technical assistance of Ms. Sheffali Dash and thoughtful comments on the manuscript from Drs. Michael Geeves and Peter Gillespie.

REFERENCES

1. Coluccio, L. M. (2008) Myosin I, in *Myosins: A superfamily of molecular motors* (Coluccio, L. M., Ed.) Springer, Dordrecht, The Netherlands.
2. Bose, A., Guilherme, A., Robida, S. I., Nicoloro, S. M., Zhou, Q. L., Jiang, Z. Y., Pomerleau, D. P., and Czech, M. P. (2002) Glucose transporter recycling in response to insulin is facilitated by myosin Myo1c. *Nature 420*, 821–824.
3. Bose, A., Robida, S., Furcinitti, P. S., Chawla, A., Fogarty, K., Corvera, S., and Czech, M. P. (2004) Unconventional myosin Myo1c promotes membrane fusion in a regulated exocytic pathway. *Mol. Cell. Biol. 24*, 5447–5458.
4. Gillespie, P. G., and Cyr, J. L. (2004) Myosin-1c, the hair cell's adaptation motor. *Annu. Rev. Physiol. 66*, 521–545.
5. Cheney, R. E., and Mooseker, M. S. (1992) Unconventional myosins. *Curr. Opin. Cell Biol. 4*, 27–35.
6. Zhu, T., Beckingham, K., and Ikebe, M. (1998) High affinity Ca^{2+} binding sites of calmodulin are critical for the regulation of myosin Ibeta motor function. *J. Biol. Chem. 273*, 20481–20486.
7. Zhu, T., Sata, M., and Ikebe, M. (1996) Functional expression of mammalian myosin I beta: analysis of its motor activity. *Biochemistry 35*, 513–522.
8. Gillespie, P. G., and Cyr, J. L. (2002) Calmodulin binding to recombinant myosin-1c and myosin-1c IQ peptides. *BMC Biochem. 3*, 31–47.
9. Cyr, J. L., Dumont, R. A., and Gillespie, P. G. (2002) Myosin-1c interacts with hair-cell receptors through its calmodulin-binding IQ domains. *J. Neurosci. 22*, 2487–2495.
10. Phillips, K. R., Tong, S., Goodyear, R., Richardson, G. P., and Cyr, J. L. (2006) Stereociliary myosin-1c receptors are sensitive to calcium chelation and absent from cadherin 23 mutant mice. *J. Neurosci. 26*, 10777–10788.
11. Manceva, S., Lin, T., Pham, H., Lewis, J. H., Goldman, Y. E., and Ostap, E. M. (2007) Calcium regulation of calmodulin binding to and dissociation from the Myo1c regulatory domain. *Biochemistry 46*, 11718–11726.
12. Adamek, N., Coluccio, L. M., and Geeves, M. A. (2008) Calcium sensitivity of the cross-bridge cycle of Myo1c, the adaptation motor of the inner ear. *Proc. Natl. Acad. Sci. U.S.A. 105*, 5710–5715.
13. Perreault-Micale, C., Shushan, A. D., and Coluccio, L. M. (2000) Truncation of a mammalian myosin I results in loss of Ca^{2+}-sensitive motility. *J. Biol. Chem. 275*, 21618–21623.
14. Clark, R., Ansari, M. A., Dash, S., Geeves, M. A., and Coluccio, L. M. (2005) Loop 1 of transducer region in mammalian class I myosin, Myo1b, modulates actin affinity, ATPase activity, and nucleotide access. *J. Biol. Chem. 280*, 30935–30942.
15. Gopalakrishna, R., and Anderson, W. B. (1982) Ca^{2+}-induced hydrophobic site on calmodulin: application for purification of calmodulin by phenyl-sepharose affinity chromatography. *Biochem. Biophys. Res. Commun. 104*, 830–836.
16. Tan, R.-Y., Mabuchi, Y., and Grabarek, Z. (1996) Blocking the Ca^{2+}-induced conformational transitions in calmodulin with disulfide bonds. *J. Biol. Chem. 271*, 7479–7483.
17. Bolton, A. E., and Hunter, W. M. (1973) The labeling of proteins to high specific radioactivities by conjugation to a ^{125}I-containing acylating agent. *Biochem. J. 133*, 529–538.
18. Glenney, J. R., and Glenney, P. (1984) The microvillus 110K cytoskeletal protein is an integral membrane protein. *Cell 37*, 743–751.
19. Pollard, T. D. (1982) Myosin purification and characterization. *Methods Cell Biol. 24*, 333–371.
20. Coluccio, L. M., and Bretscher, A. (1987) Calcium-regulated cooperative binding of the microvillar 110K-calmodulin complex to F-actin: formation of decorated filaments. *J. Cell Biol. 105*, 325–333.
21. Spudich, J. A., and Watt, S. (1971) The regulation of rabbit skeletal muscle contraction. I. Biochemical studies of the interaction of the tropomyosin-troponin complex with actin and the proteolytic fragments of myosin. *J. Biol. Chem. 246*, 4866–4871.
22. Ruppert, C., Godel, J., Müller, R. T., Kroschewski, R., Reinhard, J., and Bähler, M. (1995) Localization of the rat myosin I molecules myr 1 and myr 2 and in vivo targeting of their tail domains. *J. Cell Sci. 108*, 3775–3786.
23. Zhu, T., and Ikebe, M. (1994) A novel myosin I from bovine adrenal gland. *FEBS Lett. 339*, 31–36.
24. Reizes, O., Barylko, B., Li, C., Sudhof, T. C., and Albanesi, J. P. (1994) Domain structure of a mammalian myosin I beta. *Proc. Natl. Acad. Sci. U.S.A. 91*, 6349–6353.
25. Houdusse, A., Silver, M., and Cohen, C. (1996) A model of Ca(2+)-free calmodulin binding to unconventional myosins reveals how calmodulin acts as a regulatory switch. *Structure 4*, 1475–1490.
26. Houdusse, A., and Cohen, C. (1996) Structure of the regulatory domain of scallop myosin at 2 Å resolution: implications for regulation. *Structure 4*, 21–32.
27. Walker, R. G., Hudspeth, A. J., and Gillespie, P. G. (1993) Calmodulin and calmodulin-binding proteins in hair bundles. *Proc. Natl. Acad. Sci. U.S.A. 90*, 2807–2811.
28. Tang, N., Lin, T., Yang, J., Foskett, J. K., and Ostap, E. M. (2007) CIB1 and CaBP1 bind to the myo1c regulatory domain. *J. Muscle Res. Cell Motil. 28*, 285–291.
29. Terrak, M., Wu, G., Stafford, W. F., Lu, R., and Dominguez, R. (2003) Two distinct myosin light chain structures are induced by specific variations within the bound IQ motifs-functional implications. *EMBO J. 22*, 362–371.

BI8011059